Controlling focality and intensity of non-invasive deep brain stimulation using multipolar temporal interference in non-human primates and rodents

Boris Botzanowski[1], Emma Acerbo[1], Sebastian Lehmann[3], Sarah L. Kearsley[4], Melanie Steiner[5], Esra Neufeld[5], Florian Missey[1], Lyle Muller[4,6], Viktor Jirsa[1], Brian D. Corneil[3,4,7,8], Adam Williamson[1,2]*

[1]Institut de Neurosciences des Systèmes (INS), INSERM, UMR_1106, Aix-Marseille Université, Marseille, France
[2]International Clinical Research Center (ICRC), St. Anne's University Hospital, Brno, Czech Republic
[3]Department of Physiology and Pharmacology, Western University, London, Ontario, N6A 5B7, Canada
[4]Graduate Program in Neuroscience, Western University, London, Ontario, N6A 5B7, Canada
[5]IT'IS Foundation for Research on Information Technologies in Society, 8004 Zurich, Switzerland
[6]Department of Mathematics, Western University, London, Ontario, N6A 5B7, Canada
[7]Department of Psychology, Western University, London, Ontario, N6A 5B7, Canada
[8]Robarts Research Institute, Western University, London, Ontario, N6A 5B7, Canada

***correspondence: adam.williamson@univ-amu.fr / adam.williamson@fnusa.cz**

Abstract:

Temporal interference (TI) stimulation is a unique method of non-invasive deep brain stimulation (DBS) using transcutaneous electrodes which allows the targeting and stimulation of deeper brain structures while avoiding unwanted stimulation of shallower cortical structures. The DBS property of TI has been previously demonstrated, however, the problem of decoupling stimulation focality from stimulation intensity has not been addressed. In this paper, we directly solve the problem with a novel multipolar TI (mTI) stimulation method, which allows independent control over both the size of the stimulated region and the stimulation intensity. The mTI method uses multiple carrier frequencies to create multiple overlapping envelopes. The study presents a theoretical explanation of the concept of mTI along with experimental data gathered from Rhesus macaques and mice, permitting comparison of our technique's focality to that of the classic temporal interference stimulation technique. We show that we are able to improve the focality at depth in the brain of anesthetized mice and monkeys, and - using the new focality in awake monkeys - to evoke targeted activity, at depths never reached using non-invasive transcutaneous electrodes, namely in the superior colliculus. Finally, our results are guided and interpreted using electrodynamic simulations of mTI stimulation in a detailed monkey model.

Introduction:

During the last decade, new paradigms for non-invasive brain stimulation have been developed as promising treatments for numerous neurological diseases (schizophrenia, depression, epilepsy, etc)[1]. The primary non-invasive stimulation techniques currently in use are Transcranial Magnetic Stimulation (TMS)[2] and transcranial Current Stimulation (tCS)[3]. Using these two methods, the applied fields are shallow, as the strength of tCS is reduced as fields cross through highly resistive tissues (e.g., bone, meninges), and the strength of TMS is reduced as a function of distance from the coil. Nevertheless, both techniques reach cortical structures with sufficient strength to modulate the brain[4]. Consequently, both techniques are suited to stimulate shallow regions of the brain, but are unable to stimulate deep regions without also modulating overlying shallower regions[5,6].

In 2017, Grossman and collaborators developed a novel, non-invasive method to perform deep brain stimulation (DBS) called Temporal Interference (TI)[7]. The method simultaneously applies two high

frequency electric fields - too high to activate neurons individually - with slightly differing frequencies, thus allowing the fields to constructively and destructively interfere in time, resulting in an amplitude-modulated field. Neurons have been shown by us and by others to respond to the amplitude modulated field[8–10]. As a result, it is possible to restrict neurostimulation to the region where the two fields overlap. The restriction of the stimulated region to that overlap region is the main advantage of TI, as careful electrode placement strategies provide the ability to stimulate deep brain targets without activating overlaying regions of tissue. Using simple TI with two pairs of electrodes on the scalp we demonstrated the ability to adequately activate deep targets, such as the hippocampus[9], and to activate deep peripheral nerves, such as the sciatic and hypoglossal nerve[10,11]. However, it would be desirable to improve the focality sufficiently to target smaller brain and nerve structures – e.g., an individual nucleus of the basal ganglia. For that, tuning the size of the stimulation region and the intensity of the stimulation independently would be immensely useful, for both medical (therapeutic and diagnostic) and research applications – certainly if the size of the stimulated region could be as focal as that of implanted DBS electrodes. In the clinic, it could replace the use of certain invasive procedures such as brain mapping to identify epileptogenic region of an epileptic brain[12], or permit investigation of whether a patient will benefit from DBS prior to the implantation[13]. When coupled with non-invasive imaging techniques such as f-MRI or MEG, a non-invasive and focal stimulation technique would be an ideal way to gather data in order to build tailored, patient-specific brain models, e.g. for pre-operative planning[14]. A focal TI technique would also be a precious research tool, as it could permit access to a significantly increased number of brain areas, without the risks associated with the presence or insertion of a foreign object in the brain.

In this work, we present a non-invasive deep brain stimulation method, multipolar Temporal Interference (mTI), potentially capable of meeting the above challenges. We describe in detail the method of mTI and demonstrate the new technique with experimental data and its feasibility *in vivo* with rhesus macaques, showing non-invasive deep brain stimulation that can expand and contract the stimulation volume while maintaining the stimulation intensity. We further show that the method scales down to small animals by showing a significant increase in focality with mTI stimulation in mice. Finally, we apply this technique in an awake monkey to confirm the possibility to modulate electrophysiological activity in deep regions. We target the superior colliculus (SC), a midbrain node of the oculomotor system that moves the line of sight. The functional contribution of this structure to saccadic eye movements and the repertoire of responses that can be evoked by intracortical microstimulation are extremely well characterized[15]. Further, the oculomotor system is ideally suited to address how activity evoked by stimulation interacts with endogenous activity present at the time of stimulation[16]. We also can assess the absence of adverse reactions to stimulation by ensuring that the animal continues to perform a behavioral task during mTI. Across two behavioral tasks, we indeed show that task performance is not influenced by mTI, and we also show for the very first time that activity in the superior colliculus can be evoked using completely non-invasive transcutaneous stimulation. We expect the method to be highly useful for basic and clinical applications which employ non-invasive brain stimulation for diagnostics, therapy, and brain exploration.

Methods:

Macaque anesthetized experiment:

Ethics and animal history: Data was obtained from a male rhesus macaque monkey (*Macaca mulatta*, weighing 15 kg), as part of a planned endpoint. All surgical and experimental procedures conformed to the policies of the Canadian Council on Animal Care on the care and use of laboratory animals and were approved by the Animal Use Subcommittee of the University of Western Ontario Council. Prior to the procedure described below, the animal had a Utah array implanted in the left prefrontal cortex which had been removed 18 months earlier, as well as a pre-existing cranial implant of dental acrylic. We relied on stereotactic coordinates[17] and anatomical MRI and CT images to plan the placement of recording electrodes.

Surgical procedure and stimulation: On the day of the procedure, the animal was induced with ketamine and medatomidine, anesthetized via propofol constant rate infusion and isoflurane inhalation, and positioned in a stereotactic frame. The acrylic implant was then removed. 2-mm diameter burr-hole craniotomies were performed at pre-determined sites to permit access for Stereoelectroencephalography (sEEG) recording electrodes (Alcis Depth Coagulation Electrode). Each sEEG electrode comprised 15 recording contacts, distributed over 51 mm (contact length 2 mm, inter-contact distance 3.5 mm, diameter 0.8 mm). Eight craniotomies were positioned to permit access of recording contacts within or near the right hippocampus. A ninth craniotomy was positioned to permit access to the left hemisphere. Following each of these nine craniotomies, the sEEG electrode was lowered through a guidance screw (Alcis 2023VG, 15-25 mm length) that was secured to the skull via dental acrylic. All recording contacts were connected to an Intan recording system.

Following insertion of the sEEG electrodes, 16 locations on the scalp were selected for placement of TI stimulation electrodes. Stimulation locations were placed on the portion of the scalp that ringed the now-removed acrylic implant. The scalp was shaved and cleaned with rubbing alcohol. Stimulation was delivered through standard ECG monitoring electrodes (Medi-Trace 230, Ambu, Denmark); portions of the adhesive part of each electrode were trimmed in order to fit all electrodes on the scalp. Each electrode was connected to the output of a Digitimer DS-5 stimulator, which itself was connected to a waveform generator (Keysight EDU33212A). Connections were arranged to permit delivery of multi-pole TI through up to 4 Dipoles, forming an Octopole (8 frequencies, creating 4 overlapping envelopes).

The contact n°3 of the electrode D was chosen as the target point – thus this channel was monitored during the setting of stimulation parameters in the experiment. The current amplitudes of the 8 stimulators composing the Octopole were calibrated such that they each delivered a current resulting in a sine wave of around 750 µV peak-to-peak at the sEEG electrode (the target point), to ensure equivalence to the exposure resulting from applying 1 mA to the first Dipole. As the distance from the electrodes of a stimulator to the target was different for each stimulator, yielding a slightly different impedance, the amplitude delivered by each stimulator is necessarily slightly different to achieve the identical electrical potential at the target point. In this way, it was ensured that all electrode pairs composing the Octopole produce a field of similar amplitude at the target point. After amplitude calibration, the first stimulation Dipole (1975 and 2025 Hz) was powered and recorded. A second Dipole (2975 and 3025 Hz) was added, the phase of both signals composing the second Dipole was modified until a single 50 Hz envelope was visible (see Supplementary Figure 1). This process was repeated for the third (3975 and 4025 Hz) and fourth Dipoles (975 and 1025 Hz) to obtain the Octopole mTI. Then the fourth, third and second Dipoles were turned off and the amplitude of the first Dipole was increased to restore the initial amplitude of the 50 Hz envelope created by the Octopole.

Perfusion and CT scan: Following completion of data collection, all sEEG electrodes were cut at the top of the guide tube, and each sEEG was glued to the guide tube using medical grade silicon. The animal was then deeply anesthetized with a bolus of propofol and high percent isoflurane and euthanized through trans-cardiac perfusion with cold saline, followed by 4% PFA (performaldehyde). Care was taken during euthanasia and perfusion to ensure that the guide tubes were not disturbed, and that the sEEG electrodes remained stable within the guide tube. A post-mortem CT was performed to reconstruct the location of the sEEG electrodes, via the software MRIcroGL 1.2.20210317 x86-64.

Quantities of interest: The synchrony of responses to classic TI stimulation with the modulation frequency, as well as the phenomenologically observed steering behavior[7] (shift towards the weaker current, as the channel-current ratio changes) suggest that the envelope modulation magnitude is a suitable metric for TI stimulation, as the weaker of the two fields principally defines the modulation magnitude. However, the difference frequency is actually not part of the exposure spectrum; it only results from non-linear effects that produce frequency mixing. The lowest and therefore likely the strongest contribution results from the quadratic term (the next-higher relevant term is already fourth

order). The low frequency component is then extracted through low-pass filtering (potentially originating in the biophysics of the capacitive cellular membrane that dampens high-frequency responses). On that basis, a root-mean-square metric (with a running box-car average for 'mean') is employed to translate transient high-frequency exposure into a meaningful 'modulation envelope', the modulation amplitude of which is used as mTI exposure metric throughout this study, as seen in Figure 3. For the two channel case, the resulting metric is equivalent to the envelope obtained when fitting the peaks of the high-frequency signal. However, it generalizes naturally to more than two frequencies (mTI) and accounts for the varying oscillation density apparent when more than two channels are present.

Mock signals: Scalar signal-forms for theoretical analysis and visualization were generated by plotting simple sine functions in Matlab R2020b, such as "*sin(2*pi*frequency*t)*". Amplitude modulated signals were obtained by adding several sine functions. Note that analyses using such scalar signals are illustrative only, as in reality, the electric fields are vectorial and the transient field evolution is more complex. However, when neural responsivity is strongly dominated by a certain field orientation (e.g., fiber orientation, orientation of pyramidal neuron axis) and the projected field component along that direction can be considered relevant, the vectorial case essentially reduces to a scalar one. The field distribution illustrations in Figure 1, were created with the vector graphics software Inkscape 1.0.2-2.

Signal processing: The recordings used for the modulation index (defined as MI=1-(min/max)) analysis in Figure 1 are 0.2 second samples that are representative of the recordings at calibration point D3 for the various configurations, after phase and amplitude calibration. The recordings used for the analysis in Figure 1 were digitally filtered to keep only the high carrier frequencies and to allow an analysis of the stimulation artifacts without being influenced by physiological events or noise. For that purpose, a high-pass finite impulse response filter with a stop band of 500 Hz was applied to all signals. To highlight the high frequencies carriers, three band stop filters attenuating the power of the frequencies between 1300 and 1700, 2300 and 2700, 3300 and 3700 Hz were applied to the signals. Finally, a low pass filter of type IIR with a stop band of 4300 Hz was applied to all signals. The modulation index plotted in Figure 1 D and E was calculated from the filtered signals (see above). The signals were squared to emphasize the nonlinearity phenomenon to which the neurons are subjected. A digital low-pass filter with a stop band of 200 Hz was applied to the signal, then the square root of the real part was taken. See Appendix for a discussion on this choice of the TI exposure metric. For each parameter (Dipole and Octopole) the MI values were plotted at their respective coordinates in Figure 1 D and E. The skull was also plotted to provide spatial orientation.

Skull geometry: The skull geometry was reconstructed from a CT scan of the monkey with the software InVesalius 3.1.1 and was exported to Blender 3.1 where it was simplified through a decimation process. The top part of the skull was also removed with Boolean operations to provide a window for visualization.

Mouse experiment:

Ethics: The experiment was performed in accordance with European Council Directive EU2010/63, and French Ethics approval (Williamson, n. APAFIS#20359-2019041816357133 v10). 12-week-old OF1 mice were maintained in a transparent cage in groups of 5 mice, in a temperature-controlled room (20 ± 3°C) with a 12/12h night/day cycle. The animals had ad libitum access to food and water.

Surgical procedure: The mouse underwent a surgical procedure to implant minimally invasive screws to perform TI stimulation. The mouse was anesthetized via an intraperitoneal injection of a mix of Ketamine (50mg/Kg) and Xylazine (20mg/Kg) before being placed in a stereotaxic frame. After a midline incision, a verification that the lambda and bregma were on a horizontal plane was performed, before getting bregma coordinates. 8 pairs of minimally invasive electrodes were implanted around a multi-site depth probe (32 channels spaced by 100µm, NeuroNexus A1x32-Edge, USA). Each pair

was placed at 1mm from the depth probe [AP: -2.7, ML: +2.04, DV: 3.2]. A reference for the depth electrode has been placed in the right part of the cerebellum. Stimulation procedures occurred directly after implantation of stimulating and recording electrodes.

Electrophysiological recordings and stimulation: All electrophysiological recordings were performed with a recording/ stimulation controller (IntanTech, Intan 128ch Stimulation/Recording Controller) with a sampling rate of 30kHz. To process the data, all files have been converted from RHS format to MAT. To perform stimulation, waveform generators (Keysight, USA) were driving independent current sources (Digitimer, UK), which were stimulated via the implanted cortical electrodes. The stimulation protocol is the same as the one used in the anesthetized macaque experiment. The Octopole stimulation was realized with the following frequencies: 975|1025, 1975|2025, 2975|3025 and 3975|4025 Hz. The Dipole stimulation was realized with the frequency 1975|2025 Hz. All sets of frequencies resulted in the creation of envelopes of 50 Hz. The amplitude reached by the stimulation artifact is around 3200 µV for both Dipole and Octopole at the target contact number 16. Stimulation was continuous for each configuration.

Calculation of modulation Index: The modulation index shown in Figure 2 B was calculated in the same way as for the anesthetized macaque experiment in Figure 1 D-E.

Illustrations: The illustrations depicting the recording electrode, mouse brain, and mouse skull in Figure 2 were created using Inkscape.

Macaque awake experiment:

Ethics and animal history: Stimulation was also delivered to a different male rhesus macaque monkey (macaca mulatta, weighing 10.5 kg), during the performance of behavioral tasks. All training, surgical, and experimental procedures were in accordance with the Canadian Council on Animal Care policy on the use of laboratory animals and were approved by the Animal Use Subcommittee of the University of Western Ontario Council on Animal Care. We monitored the monkey's weight daily, and their health was under the supervision of the university veterinarian. A cranial implant of dental acrylic secured a titanium headpost, as well as a recording chamber placed over a 19-mm diameter craniotomy that permitted access to the superior colliculus. This animal had a previously implanted Utah array in the left prefrontal cortex that had been disconnected over 1 year prior to the collection of the reported data. Surgical details regarding our procedures for the preparation for SC recordings in awake behaving animals have been published previously[18,19].

Behavioral tasks: As depicted in Fig. 3A, the animal was placed with their head restrained 33 cm in front of a 42-in color monitor (4202L Elo Touch Solutions, Inc, Milpitas, CA) in a dimly-lit, sound-attenuated room. Eye movements were monitored using an ISCAN eye tracker which measures horizontal and vertical eye position as well as pupil dilation at 120 Hz. General behaviour was monitored remotely via a video camera. Visual stimuli and task behaviour were controlled by custom-built programs (MonkeyLogic[20] for Matlab), which also triggered delivery of TI and SHAM during various phases of the behavioral tasks.

The animal was trained on two tasks requiring them to look from a central fixation point to a peripheral visual target for liquid reward. Stimulation was delivered on half of all trials either during a period of active fixation (Task 1) or during saccade preparation (Task 2). For both tasks, the peripheral visual target was presented in the response field of the recorded SC neurons (~12 degrees horizontal, contralateral to the side of recording). Task 1 required the animal to look steadily at the central fixation point for a prolonged period (1900-2300ms). In the 50% of trials where stimulation was delivered, 200 ms of stimulation could start 1200-1400 ms into the fixation interval (Fig. 3B). In Task 1, stimulation was delivered when neural activity in the vicinity of the recording electrode is relatively inhibited[21], and the long fixation period facilitates measurement of pupil dilation[22,23].

In Task 2, TI stimulation was timed so that the post-stimulation interval would overlap with visual and saccadic activity related to looking to the appearing peripheral visual target, which begins about 40 ms after target presentation[24,25]. For Task 2, we reduced the central fixation interval to between 1200-1500 ms, and introduced a 100 ms gap interval between disappearance of the central fixation period and peripheral target presentation. On trials when stimulation was delivered, the 200 ms stimulation interval was timed so that it ended approximately 30 ms after target presentation, which is just before the arrival of visual information in the SC (Fig. 3C).

Stimulation and recording procedures

TI stimulation was delivered from 8 stimulators via 8 electrode pairs - specifically 16 standard ECG electrodes (Medi-Trace 230, Ambu, Denmark) arranged in a ring around the existing acrylic implant (Fig. 3A), using the same preparation procedures as described above for the anesthetized macaque experiment. Electrodes were glued to the scalp using a silicon elastomer (Kwik-Sil, World Precision Instruments). Each electrode was connected to the output of either a Digitimer DS-5 stimulator connected to a waveform generator (Keysight EDU33212A) for Task 1, or a Digitimer DS-4 stimulator connected to a Tektronix AFG1022 waveform generator for Task 2. Connections were arranged to permit delivery of multi-pole TI through up to 4 Dipoles.

Neural activity was recorded with an Intan RHS 128ch Stimulation/Recording Controller (IntanTech) system at 30kHz that also digitized at 1 kHz analog signals related to eye position, pupil dilation, and other task relevant events. To record SC activity, a 16-contact laminar electrode (Fig. 3D; S-probe, Plexon Inc, Dallas TX; 300 µm inter-electrode spacing) was lowered through a guide tube, and advanced until neural activity was encountered that was clearly related to the generation of visually-guided saccades. Since the electrode approached the SC in a surface-normal manner, functionally-related activity was seen across multiple channels that spanned the superficial and intermediate layers of the SC (Supplementary Fig. S2). Prior to data collection, a contact that was clearly in the intermediate layers of the SC was chosen as the calibration point (e.g., Fig. 3D), and as before, each electric field was calibrated so each would deliver a current resulting in a sine wave of ~200 µV at that calibration point. The phases of each Dipole were then aligned at the calibration point. The currents were then increased by a common value, to a point below that which provoked any responses to stimulation (i.e., scalp twitches or blinks).

During data collection, two blocks of trials were run. In the first block of trials, trials with Octopole multipolar TI stimulation with a 100-Hz envelope were intermixed with trials without stimulation at equal rates (i.e., 50% TI stimulation and 50% no stimulation trials). In the second block of trials, SHAM TI stimulation trials were intermixed with no stimulation trials (i.e., 50% SHAM stimulation and 50% no stimulation trials). SHAM stimulation was delivered by either turning off half of the stimulators (Task 1; Fig. 3B), or by equalizing the carrier frequencies within a given Dipole, removing any TI envelope (Task 2; Fig. 3C).

Multi-unit neural spiking activity was sorted offline in principal component space after manual threshold setting (Offline Sorter, Plexon Inc., USA), and further analysed with Matlab (MathWorks Inc, USA). For firing rate visualization, spike times were convolved with an excitatory post-synaptic potential spike function[19,26] and rasters and trial-averaged spike density functions were plotted using the Matlab toolbox Gramm[27]. Due to the artifact during the stimulation interval, we focus on spiking activity immediately following stimulation offset, as neural activity has been shown to be commonly modulated in this interval during various forms of non-invasive brain stimulation in behaving non-human primates[28,29].

Results:

Multipolar temporal interference principle:

Multipolar TI (mTI) creates a non-invasive DBS with the potential to have focality approaching intracranial DBS resolution and is conceptually presented in Figure 1 along with preliminary results in one rhesus macaque. As illustrated in Figure 1A, standard TI creates deep subcortical stimulation by a combination of two kHz frequencies applied through two pairs of electrodes, where the field from the first pair (red) and the field from the second pair (light red) overlap to create a region with strong envelope modulation (yellow). The frequency of the envelope is equal to the difference between the two kHz frequencies and is set to a value equal to a frequency from traditional deep brain stimulation to be non-invasively replicated – for example in the hippocampus 50Hz for excitation or 130Hz for inhibition in accordance with our previous publications on TI stimulation in epilepsy[13]. Neural activity can only be influenced in the region of overlap, where a significant low-frequency envelope results, as the minimally modulated kHz exposure outside that region does not efficiently drive neuronal activity. Unfortunately, the focality of standard TI stimulation (the size of the yellow overlap region in the schematic representation) cannot be adapted independently from the intensity of the stimulation (the maximum value of the envelope); for example, in Figure 1A, the size of the yellow region cannot simply be decreased to a four times smaller spot while maintaining the same amplitude. The problem is resolved by mTI (Figure 1B).

As illustrated in Figure 1B, mTI utilizes combinations of TI exposures that have different frequency carriers, but overlapping regions of strong modulation, such that the strongly modulated region of their sum is restricted to that overlap, while modulation is diluted elsewhere – similarly to the concept of field multiplexing in hyperthermia therapy[30]. As a result, mTI can independently adapt size and intensity. When the intensity of the stimulation from the four pairs of electrodes (red, light red, green, light green) is decreased until the peak envelope amplitude reaches that of two channel TI, focality increases (the yellow region is now smaller, but has the same intensity as the original yellow region).

Demonstration of focality gain using mTI in a macaque

As seen in Figure 1D, standard TI is performed in an anesthetized macaque monkey. Two pairs of electrodes provided two frequencies. The envelope amplitude is depicted using the modulation index (the amount of amplitude modulation; again yellow is the highest). Numerous sEEG electrode recordings in the macaque show that the stimulation is subcortical, but not particularly focal. As seen in Figure 1E, mTI is performed to increase the focality compared to standard TI (8 pairs of electrodes providing 8 frequencies, creating an Octopole, with 4 overlapping envelopes). As evident in the macaque measurements, the focality increases: the yellow region is now much smaller, but has the same intensity as the original yellow region.

Focality gain using mTI scales to smaller animals

As depicted in Figure 2A, standard TI was performed in the mouse and compared to mTI. In Figure 2B, two pairs of electrodes provided currents at two frequencies and the envelope amplitude is again depicted using the modulation index. It is not possible to implant numerous SEEG electrodes in the mouse, therefore a silicon depth probe was implanted through the hippocampal target. The 32 electrodes do not show important variations in modulation index for this electrode configuration, indicating that for the given exposure configuration the stimulation reaches the hippocampal target but is not particularly focal. As further seen in Figure 2B, mTI (8 pairs of electrodes providing 8 frequencies generating 4 overlapping envelopes) increases the focality compared to standard TI. Similarly, to what the previous figure shows, the focality significantly increases, as evidenced by the reduction of modulation index outside of the hippocampal target (around electrode 16 and below).

Activity evoked by multipolar temporal interference stimulation in an awake macaque

To further study the possibility of inducing an electrophysiological response, we delivered mTI stimulation to the subcortical midbrain superior colliculus (SC) in an awake macaque engaged in a prolonged period of active visual fixation (Task 1, Fig. 3B), or just before the generation of a visually-guided saccade (Task 2; Fig. 3C). Simultaneously, we recorded activity from SC via a linear array electrode positioned to span the superficial and intermediate areas of the SC. mTI stimulation was focused on an intermediate contact on the linear array from which functionally-related activity was recorded (e.g., Supplementary Figure S2). For both Tasks, one block of trials consisted of Octopole mTI stimulation intermixed with no-stimulation trials, and another block of trials consisted of SHAM mTI stimulation intermixed with no-stimulation trials (see Fig. 3B, C for frequencies delivered). For these experiments, we created a controllable burst of envelopes of 100 Hz with four pairs of high frequency carriers offset by a common amount (Fig. 3E,F; f1=1950|2050 Hz, f2=3950|4050, f3=5950|6050 Hz, and f4=7950|8050 Hz). Simulations (Fig. 3G) confirm the increase in focality when targeting the SC with this electrode configuration, by first simply visualizing the amplitude of the envelope's electric field using iso-surfaces (red) where the electric field along the surface is equal, 6V/m in these specific images. Clearly the mTI is more focal than the standard TI. Additionally, the cumulative histogram is instructive, where the electric field in the target SC is plotted with respect to the electric field in the rest of the simulated tissue. The electric field in the SC is highlighted, with less than approximately 1% of brain tissue receiving a higher electric field. In contrast, for TI, approximately 20% of brain tissue is receiving a higher electric field. The high frequency carriers are shown for clarity, where compared to the colliculus, approximately 40% of brain tissue is receiving a higher electric field, which is understandable as the highest electric field from the carriers is found nearest to the stimulation electrodes.

Our choice of the SC as our subcortical target is based on its well-characterized activity patterns before visually-guided saccades[24,25], and on the saccadic and non-saccadic effects that can be provoked by intracortical microstimulation at 100 Hz[22,31,32]. We positioned the recording electrode in the vicinity of neurons within the intermediate layers of the SC that are recruited prior to the generation of visually-guided saccades. In both Tasks, we saw no evidence that either Octopole mTI or SHAM TI distracted the animal or interfered with their ability to perform the tasks. We also saw no evidence that stimulation evoked any visible discomfort, scalp twitches, or blinking responses.

In both Tasks, we were unable to reliably resolve SC activity during the stimulation interval. Accordingly, we focus on the patterns of activity in the period immediately after stimulation offset. For the data shown from Task 1 (the active fixation task), the example neuron was clearly recruited during the generation of leftward visually-guided saccade (Supplementary Figure S2). As expected for such a neuron, we observed only a low-level of tonic activity during a period of active fixation (black traces in Fig. 4A). Notably, the activity of this SC neuron increased for ~150 ms following Octopole mTI (red rasters and spike density functions in Fig. 4A). Such a post-stimulation increase in activity was not seen on trials without stimulation (black rasters and spike density functions in Fig. 4A), nor on trials SHAM TI trials where one of each Dipole delivered a carrier frequency (blue rasters and spike density functions in Fig. 4A). Behaviorally, Octopole mTI stimulation did not evoke any eye movements (top rows, Fig. 4A). However, Octopole mTI stimulation did induce pupil dilation (2nd row, Fig. 4A, red traces), which is broadly consistent with stimulation of the intermediate SC that is below the level required to provoke saccades[22]. Pupil dilation, albeit to a smaller degree, was also provoked by SHAM TI stimulation (2nd row, Fig. 4A, blue traces). This latter result emphasizes the need for future controls of sensory percepts that may arise from the carrier frequencies. Repeating similar mTI delivery in human participants would also allow for the reporting of sensations arising from stimulation.

We also studied the ability of mTI to influence functionally-related activity. On another day, our recording electrode was again positioned to record prominent saccade-related activity (see no-

stimulation data shown by black rasters and spike density functions in Fig. 4B). Such functionally-related activity increased for ~50 ms following Octopole (100 Hz envelope) mTI stimulation (red rasters and spike density functions in Fig. 4B), but did not increase following SHAM TI stimulation where all electrodes delivered high carrier frequency without any offset (blue rasters and spike density functions in Fig. 4B). We did not observe any influence of Octopole mTI on saccadic reaction time, although this may be due to the relatively low number of trials in each condition.

Discussion

In this work, we have shown the feasibility of creating extensively customizable and steerable non-invasive deep brain stimulation, where the size of the deep brain target and the intensity of stimulation can be tuned independently. Specifically, the superposition of multiple, spatially-distinct TI-modulation regions at a single brain target was demonstrated in both non-human primates and rodents, creating a single aggregate envelope with an exposure magnitude significantly greater than that of the individual contributing fields. Using overlapping electric fields allowed us to increase the focality of stimulation because although the multiple electric fields intersect at the same brain target, the current paths associated with the multiple contributing pairs differ, ensuring that off-target regions of significant TI modulation are distinct and diluted in average. Thus a local maximum at the targeted point can be sustained while reducing the modulation index elsewhere. This is evident in Figure 1 and 2.

The impact of TI and mTI on intracranial electrophysiological activity was further demonstrated by the post-stimulation increase in activity in the SC of an awake behaving non-human primate. To our knowledge, this is the first time that neural effects of non-invasive stimulation of the primate SC, achieved here with mTI, have been demonstrated. Given the topographic organization of the intermediate layers of the SC, future studies may be able influence specific saccade vectors by changing the focus of stimulation. mTI stimulation of the SC also provoked pupil dilation. While encouraging, we are mindful that SHAM TI stimulation also provoked pupil dilation, albeit to a lesser degree. These results emphasize the need for careful behavioral controls for percepts arising from mTI in the future. Further, other work has shown that the magnitude of pupil dilation evoked by intracortical microstimulation of the SC is coordinated with subsequent saccade behavior[33]; examining whether something similar happens with mTI would also help differentiate between specific effects of mTI at the SC versus generic effects arising from sensory percepts. The feasibility of such future experiments is bolstered by our data collected to date that mTI stimulation does not cause blinking nor disrupt task performance, as could have been expected if mTI were to cause any adverse reactions.

The results presented here clearly have applications well beyond the stimulation targets explored in this work. A non-invasive method of electrical stimulation, which simultaneously expanded the amount of explorable tissue by allowing access to regions previously difficult or unavailable to traditional invasive implants would offer clear and immediate clinical benefits to patients and surgeons, e.g., for (i) the identification of personalized locations of increased safety and efficacy for long-term therapeutic implants and (ii) state-of-the-art applications that suppress epileptic activity for prolonged periods, potentially creating permanent brain seizure immunity.

The non-invasive focal stimulation described here has a clear application for personalization and addresses fundamental needs of brain stimulation in brain health applications in general, – the need for less invasive, more targeted treatments. Therefore, it will clearly be relevant and highly exploitable for numerous other brain diseases such as depression, Parkinson's, Alzheimer's, and other neuropathological conditions which regularly utilize stimulation, continuous or intermittent transcutaneous electrical stimulation.

Funding information: This work was funded in part by operating grants to BDC from the Canadian Institutes of Health Research (CIHR; MOP-93796, MOP-123247), an Accelerator Grant to BDC and

LM from the Canada First Research Excellence Fund (BrainsCAN), and an institutional support grant to BDC from Western University. SLK was supported by graduate awards from the Natural Sciences and Engineering Research Council of Canada (CGS-M), the Ontario Government, and the Parkinson Society Southwestern Ontario and MITACS.

This research was supported by funds from the European Research Council (ERC) under the European Union's Horizon 2020 research and innovation program (grant agreement starting grant No. 716867 and POC No 963976).

Figure 1. Principle of multipolar temporal interference and increased focality in non-human primates
A. TI: Adding two frequencies to create an envelope – Two equal amplitude sinusoidal signals at 1975 Hz and 2025 Hz interact to create a 50 Hz amplitude modulated signal.
B. mTI: **Adding two envelopes to create a greater envelope** – The first 50 Hz amplitude modulated signal is created from the interaction of 1975 and 2025 Hz signals, the second from 2975 and 3025 Hz. When these two are summed, they create a larger 50 Hz exposure, forming a spatial quadrupole.
C. mTI: Reducing the amplitude to that of the original TI envelope increases focality – The left panel is the temporal signal of classic TI (from A). The middle panel is the larger summed signal (from B). When the amplitude from the electrode pairs in is reduced to match the original TI envelope amplitude, the focality can dramatically increase.
D. Classic TI and measurements a macaque monkey – The region of strong amplitude modulation is found to be subcortical with TI using two high frequencies currents, but the focality is limited.
E. mTI and measurements in a macaque monkey – The focality of region of strong amplitude modulation from D is significantly improved with mTI using 8 frequencies to create 4 intersecting modulation regions. The magnitude of the combined exposure of these overlapping fields is decreased to match that of the hippocampal TI exposure (measured at the contact indicated by a red arrow). This results in a much more focal hippocampal stimulation.

Figure 2. Increased Focality in rodents
A. Experimental mouse set up – Position of the recording electrodes in the mouse brain [AP: -2.7, ML: +2.04, DV: 3.2]. Plots of raw recording from electrode n°16 (highlighted in red) for Dipole and Octopole configurations.
B. Spatial distribution of Modulation Index – Shallow (electrode 26 - blue) and deep contacts (electrode 7 - yellow) are highlighted to facilitate localization in the modulation index plots. The maximal modulation index for both Dipole and Octopole configuration is reached in the hippocampus (approximately electrode 16 – red). However, the focality is clearly greater in the mTI (Octopole) configuration. When comparing these results with those from the previous and subsequent figures, we conclude that mTI scales well between larger and smaller anatomical geometries.

Figure 3. mTI layout, behavioral paradigm, and simulations in the awake behaving macaque
A. Experimental setup. Sketch of the placement of scalp-based stimulation electrodes ringing the acrylic implant, in which the SC recording chamber was embedded. The stimulation electrodes are color coded and connected by colored lines to show the Dipole pairs for the octo-pole.
B,C. Behavioral tasks. 200 ms of mTI stimulation was embedded either within a visually-guided saccade task where stimulation was either delivered during a period of prolonged visual fixation (Task 1) or around the time of target onset in a visually-guided saccade task (Task 2). We also show the settings of the carrier frequencies for the delivery of Octopole mTI stimulation or SHAM stimulation.
D. Focusing mTI. An intermediate contact on the linear electrode array (shown in red) located within the intermediate SC was selected to be the point for mTI calibration and phase alignment.
E. Spectrogram of signal - Frequencies used for the stimulation and the corresponding Dipole. For this experiment, a 100 Hz envelope was used to evoked activity. Pairs with higher frequencies were placed closer to the animal face due to the less sensations on the skin provoked.

F. PSD of signal - Time frequency and periodogram of one of the 200ms of TI – here only Octopole is displayed-. The different frequencies applied are visible and a lowpass filter <100Hz is enough to get rid of the artefact of stimulation on the recorded data.

G. Sim4Life simulations of TI and mTI stimulation. Iso-surface in red showing 6 V/m, everything inside the surface is 6V/m or higher. Clearly the iso-surface from mTI is significantly more focal than that from TI. Furthermore, the cumulative histogram shows the normalized maximum electric field in the target superior colliculus vs percentage of brain coverage. Very clearly for the mTI (orange), less than 1 percent of the brain receives an electric field higher than the electric field in the colliculus. For the TI (blue), more than 20 percent of the brain receives an electric field higher than the electric field in the colliculus. For context, we see that 40 percent of the brain receives a higher electric field from the high frequency carriers (yellow), which is to be expected as the carrier frequency maximum is closest to the electrodes providing the carrier.

Figure 4. Examples of mTI on spiking activity in the superior colliculus (SC) in the awake, behaving macaque A) Effects of mTI during a period of stable visual fixation. mTI did not influence eye position (horizontal gaze position, top row), but did increase SC activity (red rasters and spike density functions). Such an increase in activity was not observed on no-stimulation trials (grey and black rasters and spike density functions), nor on SHAM stimulation trials (blue rasters and spike density functions). In addition, mTI induced pupil dilation (middle row) that was absent in no-stimulaton trials and more prominent than on SHAM stimulation trials. Contours show mean subtended by the standard error of the mean.

B) Effects of mTI delivered before a visually-guided saccade. When delivered just before the arrival of visual information in the SC in a visually-guided saccade task, mTI provoked a post-stimulation increase in functionally-related activity (red rasters and spike density functions) that was not observed on no-stimulation trials (black traces and spike density functions) nor on SHAM stimulation trials (blue traces and spike density functions).

Supplementary Figure 1. Phase interactions in a multipole

Just like the two high-frequency carriers ('Dipole') interfere temporally in classic TI to create a low-frequency modulation envelope, multiple such Dipoles with strongly different carrier frequencies interfere to create a more complex envelope shape. However, while the envelope shape is unaffected by the relative phase in the two-channel case (only its phase is), the envelope shape has a complex dependence on the underlying phases when more than two frequencies are present. Special care must therefore be taken to ensure that the multiple Dipoles are in phase at the calibration point. The different plots here represent a case of perfect phase tuning (left), a case where the two envelopes are phased such that their combination is hardly modulated (right) and a case in between (middle).

Supplementary Figure 2: Example of functionally-related neural activity recorded from the SC

Spiking activity of the unit shown in Fig. 4A of the main manuscript, focusing here on the activity following visual target onset. Top left panel shows eye movement trajectories for three 12 deg saccade vectors directed contralateral to the side of SC recording, with the color scheme denoting different vertical components. Middle to bottom left panels show, using the same color scheme, the horizontal eye position traces (downward deflections denote left movements), the rasters of neural activity recorded from a channel in the intermediate layers of the SC, highlighted in red in the middle column, and the associated spike density functions. Middle column shows spike density functions for those channels positioned within the intermediate layers of the SC.

References

1. Wagner, T., Valero-Cabre, A. & Pascual-Leone, A. Noninvasive human brain stimulation. *Annu Rev Biomed Eng* **9**, 527–565 (2007).
2. Klomjai, W., Katz, R. & Lackmy-Vallée, A. Basic principles of transcranial magnetic stimulation (TMS) and repetitive TMS (rTMS). *Annals of Physical and Rehabilitation Medicine* **58**, 208–213 (2015).
3. Roy, A. V., Camchong, J. & Lim, K. O. Principles and Applications of Transcranial Electrical Stimulation. in *Engineering in Medicine* 319–334 (Elsevier, 2019). doi:10.1016/B978-0-12-813068-1.00012-9.
4. Rossini, P. M. *et al.* Non-invasive electrical and magnetic stimulation of the brain, spinal cord, roots and peripheral nerves: Basic principles and procedures for routine clinical and research application. An updated report from an I.F.C.N. Committee. *Clin Neurophysiol* **126**, 1071–1107 (2015).
5. Deng, Z.-D., Lisanby, S. H. & Peterchev, A. V. Electric field depth-focality tradeoff in transcranial magnetic stimulation: simulation comparison of 50 coil designs. *Brain Stimul* **6**, 1–13 (2013).
6. Mikkonen, M., Laakso, I., Tanaka, S. & Hirata, A. Cost of focality in TDCS: Interindividual variability in electric fields. *Brain Stimulation* **13**, 117–124 (2020).
7. Grossman, N. *et al.* Noninvasive Deep Brain Stimulation via Temporally Interfering Electric Fields. *Cell* **169**, 1029-1041.e16 (2017).
8. Acerbo, E. *et al.* Focal non-invasive deep-brain stimulation with temporal interference for the suppression of epileptic biomarkers. *Front Neurosci* **16**, 945221 (2022).
9. Florian, M. *et al.* Orientation of Temporal Interference for Non-invasive Deep Brain Stimulation in Epilepsy. *Frontiers in Neuroscience* **15**, 633988 (2021).
10. Botzanowski, B. *et al.* Noninvasive Stimulation of Peripheral Nerves using Temporally-Interfering Electrical Fields. *Advanced Healthcare Materials* **11**, 2200075 (2022).

11. Missey, F. *et al.* Obstructive sleep apnea improves with non-invasive hypoglossal nerve stimulation using temporal interference. *Bioelectron Med* **9**, 18 (2023).
12. George, D. D., Ojemann, S. G., Drees, C. & Thompson, J. A. Stimulation Mapping Using Stereoelectroencephalography: Current and Future Directions. *Front. Neurol.* **11**, 320 (2020).
13. Acerbo, E. *et al.* Focal non-invasive deep-brain stimulation with temporal interference for the suppression of epileptic biomarkers. *Frontiers in Neuroscience* **16**, (2022).
14. Ritter, P., Schirner, M., McIntosh, A. R. & Jirsa, V. K. The virtual brain integrates computational modeling and multimodal neuroimaging. *Brain Connect* **3**, 121–145 (2013).
15. Gandhi, N. J. & Katnani, H. A. Motor functions of the superior colliculus. *Annu Rev Neurosci* **34**, 205–231 (2011).
16. Lehmann, S. J. & Corneil, B. D. Completing the puzzle: Why studies in non-human primates are needed to better understand the effects of non-invasive brain stimulation. *Neurosci Biobehav Rev* **132**, 1074–1085 (2022).
17. Paxinos, G., Huang, X.-F. & Toga, A. The Rhesus Monkey Brain in Stereotaxic Coordinates. *Faculty of Health and Behavioural Sciences - Papers (Archive)* (2000).
18. Rezvani S & Corneil Bd. Recruitment of a head-turning synergy by low-frequency activity in the primate superior colliculus. *Journal of neurophysiology* **100**, (2008).
19. Peel, T. R., Dash, S., Lomber, S. G. & Corneil, B. D. Frontal Eye Field Inactivation Diminishes Superior Colliculus Activity, But Delayed Saccadic Accumulation Governs Reaction Time Increases. *J Neurosci* **37**, 11715–11730 (2017).
20. Hwang, J., Mitz, A. R. & Murray, E. A. NIMH MonkeyLogic: Behavioral control and data acquisition in MATLAB. *J Neurosci Methods* **323**, 13–21 (2019).
21. Munoz, D. P. & Fecteau, J. H. Vying for dominance: dynamic interactions control visual fixation and saccadic initiation in the superior colliculus. *Prog Brain Res* **140**, 3–19 (2002).
22. Wang, C.-A., Boehnke, S. E., White, B. J. & Munoz, D. P. Microstimulation of the monkey superior colliculus induces pupil dilation without evoking saccades. *J Neurosci* **32**, 3629–3636 (2012).

23. Lehmann, S. J. & Corneil, B. D. Transient Pupil Dilation after Subsaccadic Microstimulation of Primate Frontal Eye Fields. *J Neurosci* **36**, 3765–3776 (2016).
24. Goldberg, M. E. & Wurtz, R. H. Activity of superior colliculus in behaving monkey. I. Visual receptive fields of single neurons. *J Neurophysiol* **35**, 542–559 (1972).
25. Wurtz, R. H. & Goldberg, M. E. Activity of superior colliculus in behaving monkey. 3. Cells discharging before eye movements. *J Neurophysiol* **35**, 575–586 (1972).
26. Thompson, K. G., Hanes, D. P., Bichot, N. P. & Schall, J. D. Perceptual and motor processing stages identified in the activity of macaque frontal eye field neurons during visual search. *J Neurophysiol* **76**, 4040–4055 (1996).
27. Morel, P. Gramm: grammar of graphics plotting in Matlab. *Journal of Open Source Software* **3**, 568 (2018).
28. Mueller, J. K. *et al.* Simultaneous transcranial magnetic stimulation and single-neuron recording in alert non-human primates. *Nat Neurosci* **17**, 1130–1136 (2014).
29. Romero, M. C., Davare, M., Armendariz, M. & Janssen, P. Neural effects of transcranial magnetic stimulation at the single-cell level. *Nat Commun* **10**, 2642 (2019).
30. Poni, R., Neufeld, E., Capstick, M., Bodis, S. & Kuster, N. Rapid SAR optimization for hyperthermic oncology: combining multi-goal optimization and time-multiplexed steering for hotspot suppression. *Int J Hyperthermia* **39**, 758–771 (2022).
31. Stanford, T. R., Freedman, E. G. & Sparks, D. L. Site and parameters of microstimulation: evidence for independent effects on the properties of saccades evoked from the primate superior colliculus. *J Neurophysiol* **76**, 3360–3381 (1996).
32. Corneil, B. D., Olivier, E. & Munoz, D. P. Neck muscle responses to stimulation of monkey superior colliculus. I. Topography and manipulation of stimulation parameters. *J Neurophysiol* **88**, 1980–1999 (2002).
33. Wang, C.-A. & Munoz, D. P. Coordination of Pupil and Saccade Responses by the Superior Colliculus. *J Cogn Neurosci* **33**, 919–932 (2021).

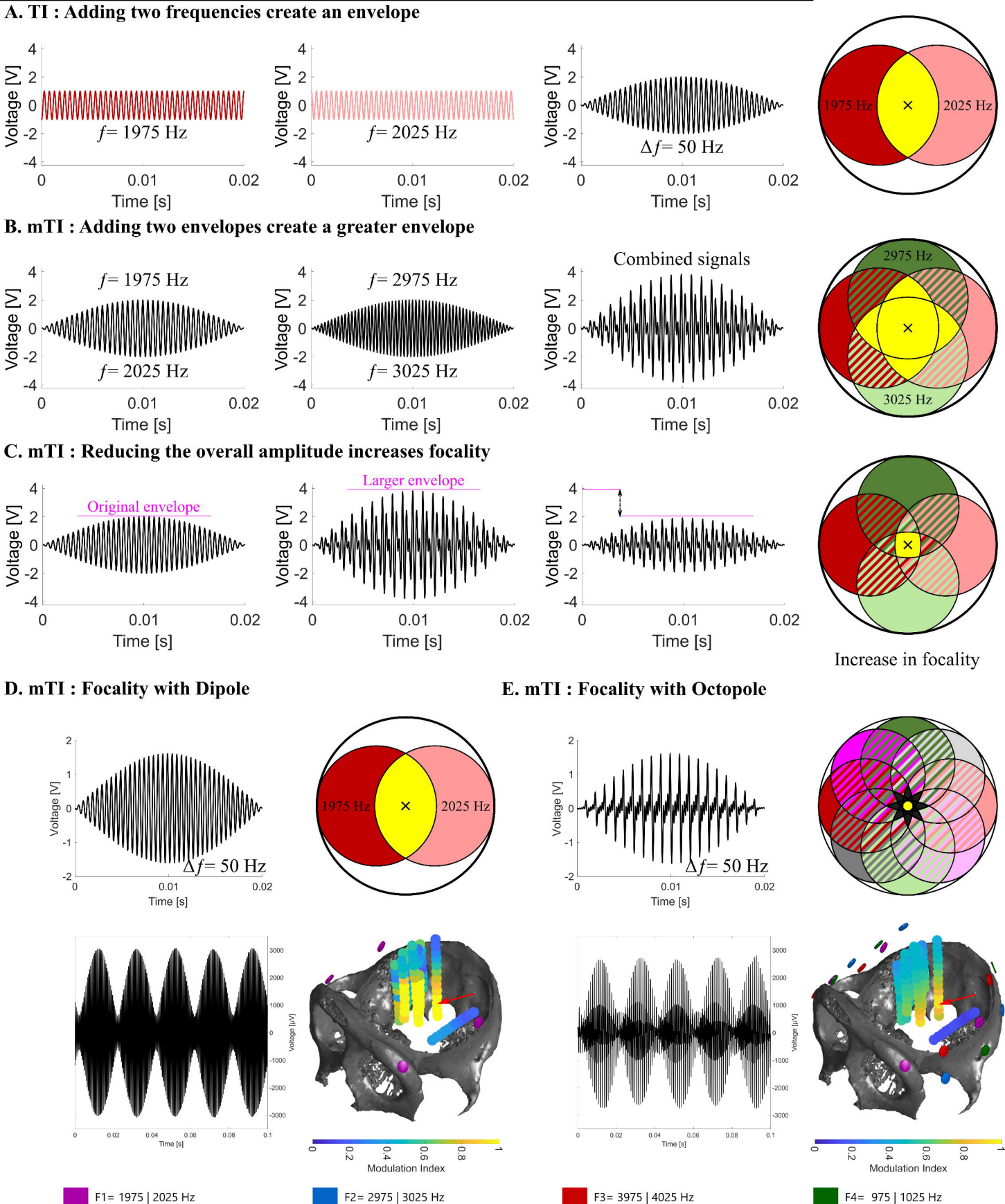
A. TI : Adding two frequencies create an envelope
f= 1975 Hz
f= 2025 Hz
Δf= 50 Hz
1975 Hz
2025 Hz
B. mTI : Adding two envelopes create a greater envelope
f= 1975 Hz
f= 2025 Hz
f= 2975 Hz
f= 3025 Hz
Combined signals
2975 Hz
3025 Hz
C. mTI : Reducing the overall amplitude increases focality
Original envelope
Larger envelope
Increase in focality
D. mTI : Focality with Dipole
E. mTI : Focality with Octopole
Voltage [V]
Time [s]
Voltage [μV]
Modulation Index
F1= 1975 | 2025 Hz
F2= 2975 | 3025 Hz
F3= 3975 | 4025 Hz
F4= 975 | 1025 Hz

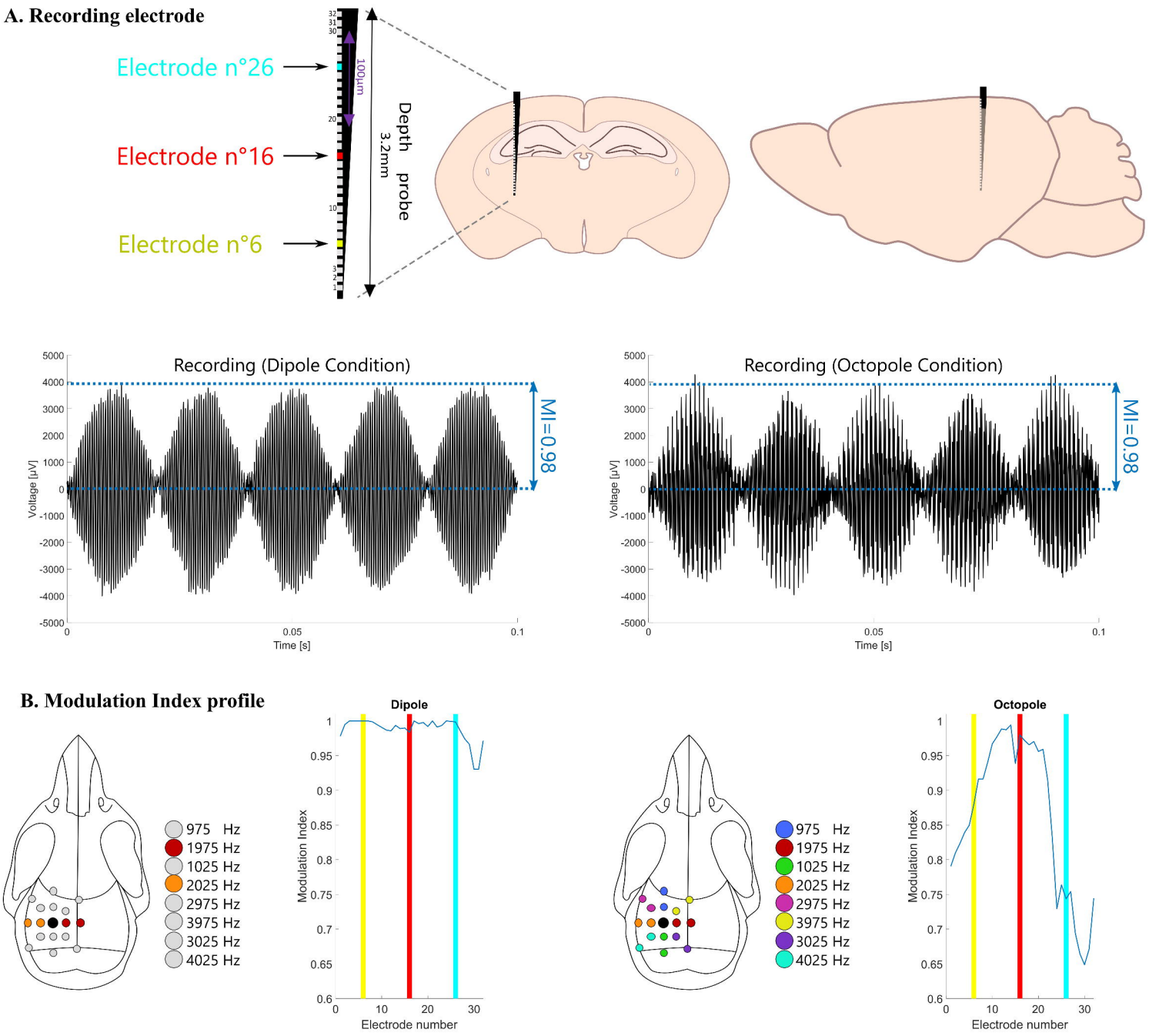
A. Recording electrode
Electrode n°26
Electrode n°16
Electrode n°6
100µm
Depth probe
3.2mm
Recording (Dipole Condition)
Recording (Octopole Condition)
MI=0.98
Voltage [µV]
Time [s]
B. Modulation Index profile
Dipole
Octopole
975 Hz
1975 Hz
1025 Hz
2025 Hz
2975 Hz
3975 Hz
3025 Hz
4025 Hz
Modulation Index
Electrode number

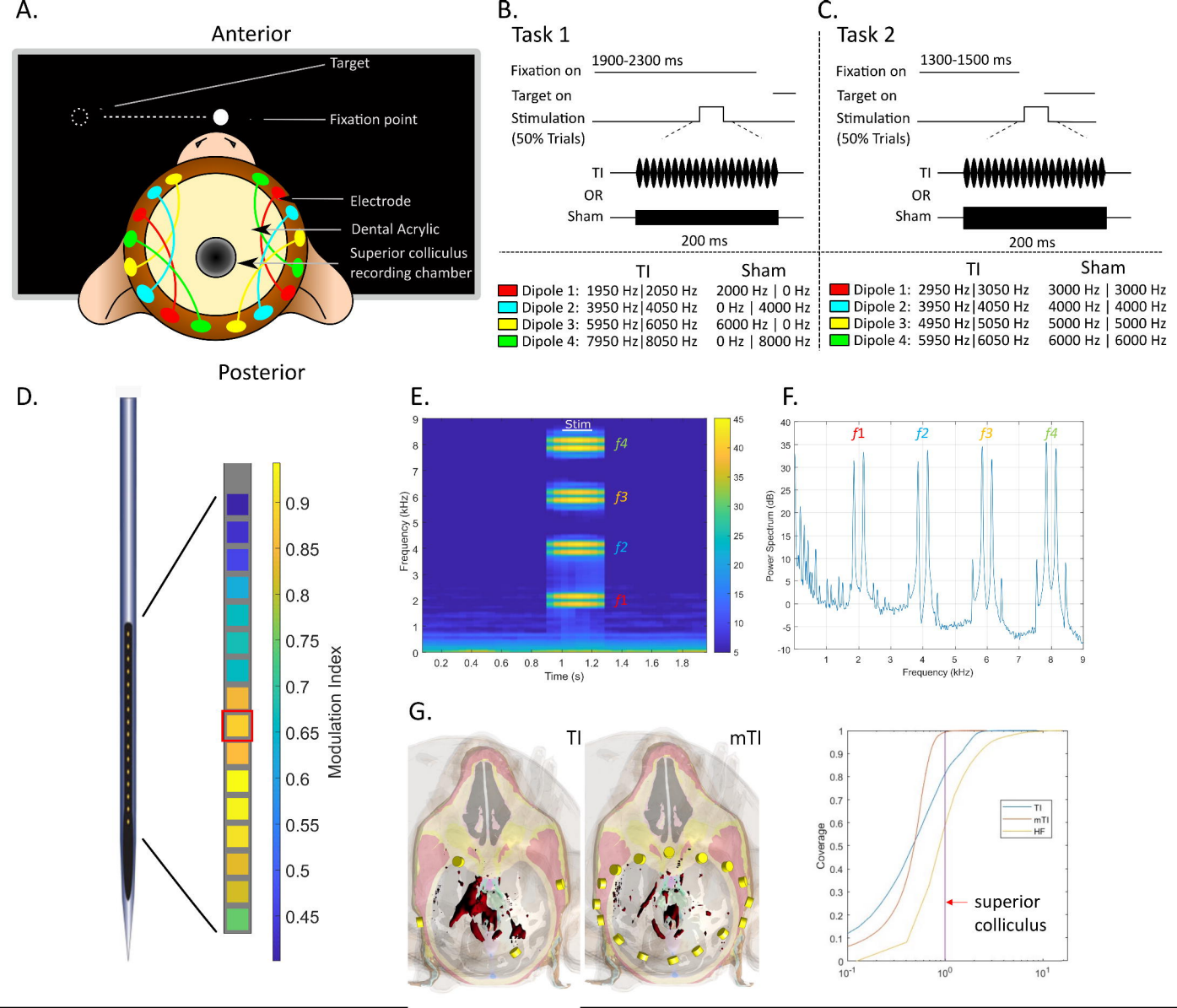
A.
Anterior
Target
Fixation point
Electrode
Dental Acrylic
Superior colliculus
recording chamber
B.
Task 1
Fixation on
1900-2300 ms
Target on
Stimulation
(50% Trials)
TI
OR
Sham
200 ms
TI
Sham
Dipole 1: 1950 Hz | 2050 Hz
2000 Hz | 0 Hz
Dipole 2: 3950 Hz | 4050 Hz
0 Hz | 4000 Hz
Dipole 3: 5950 Hz | 6050 Hz
6000 Hz | 0 Hz
Dipole 4: 7950 Hz | 8050 Hz
0 Hz | 8000 Hz
C.
Task 2
Fixation on
1300-1500 ms
Target on
Stimulation
(50% Trials)
TI
OR
Sham
200 ms
TI
Sham
Dipole 1: 2950 Hz | 3050 Hz
3000 Hz | 3000 Hz
Dipole 2: 3950 Hz | 4050 Hz
4000 Hz | 4000 Hz
Dipole 3: 4950 Hz | 5050 Hz
5000 Hz | 5000 Hz
Dipole 4: 5950 Hz | 6050 Hz
6000 Hz | 6000 Hz
Posterior
D.
0.9
0.85
0.8
0.75
0.7
0.65
0.6
0.55
0.5
0.45
Modulation Index
E.
Stim
f4
f3
f2
f1
Frequency (kHz)
Time (s)
F.
f1
f2
f3
f4
Power Spectrum (dB)
Frequency (kHz)
G.
TI
mTI
Coverage
TI
mTI
HF
superior
colliculus

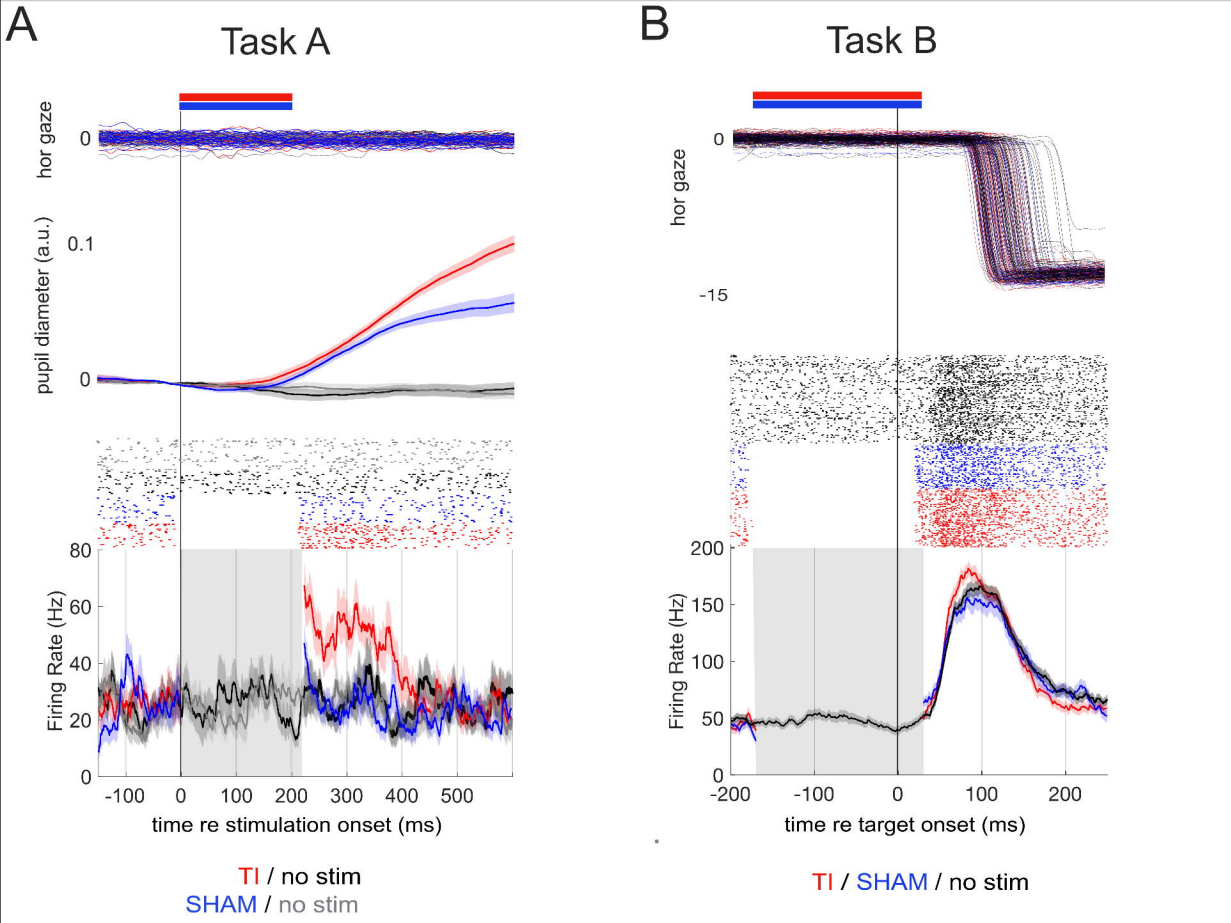
A
Task A
hor gaze
0
pupil diameter (a.u.)
0.1
0
Firing Rate (Hz)
80
60
40
20
0
-100
0
100
200
300
400
500
time re stimulation onset (ms)
TI / no stim
SHAM / no stim
B
Task B
hor gaze
0
-15
Firing Rate (Hz)
200
150
100
50
0
-200
-100
0
100
200
time re target onset (ms)
TI / SHAM / no stim

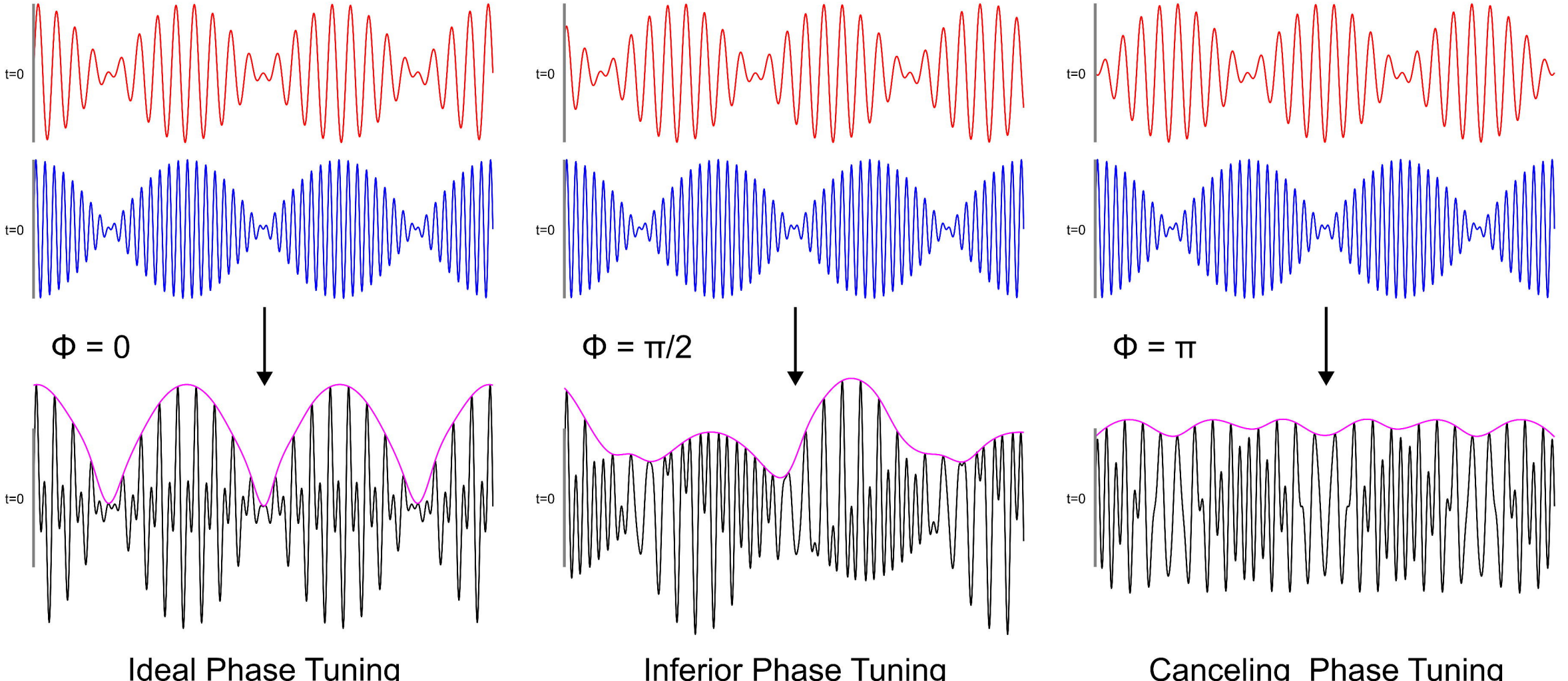
t=0
t=0
Φ = 0
t=0
Ideal Phase Tuning
t=0
t=0
Φ = π/2
t=0
Inferior Phase Tuning
t=0
t=0
Φ = π
t=0
Canceling Phase Tuning